ORIGINAL PAPER

High-pressure shift freezing: recrystallization during storage

Pedro P. Fernández · Laura Otero ·
Miriam M. Martino · Antonio D. Molina-García ·
Pedro D. Sanz

Abstract High-pressure shift freezing has been proposed as a method to produce frozen food with smaller ice crystal size and, consequently, with reduced tissular damage and higher overall quality. The fate of this initially improved crystal size distribution, decisive for the long-term value of this procedure, is unclear. The recrystallization behaviour of partially frozen aqueous solutions, as food models, is here compared with that of similar classically frozen samples. A microscopic observation cell has been specially designed for this purpose. The temporal evolution of high-pressure shift frozen ice crystals has been fitted to different mechanism models and is found to be similar within experimental error to that of classically frozen samples. However, differences in the shape evolution of crystals have been detected, which can be ascribed to small differences in the initial distribution. The implications of these observations for the long-term storage of frozen food are discussed.

Keywords High-pressure shift freezing · HPSF · Frozen storage · Ice crystal · Recrystallization · Ostwald ripening

P. P. Fernández · L. Otero · A. D. Molina-García (✉) ·
P. D. Sanz
Instituto del Frío (CSIC), José Antonio Novais 10,
28040 Madrid, Spain
e-mail: ifrm111@if.csic.es

M. M. Martino
Centro de Investigación y Desarrollo en Criotecnología de Alimentos (C·I.D.C.A.), CONICET Facultad de Ciencias Exactas y Facultad de Ingeniería, Universidad Nacional de La Plata, calle 47 y 116 (1900), La Plata, Argentina

Introduction

Freezing is extensively used for the preservation of food and other biological specimens, as it keeps most quality-related parameters virtually unaltered for long periods. However, the final quality of the product (aspects such as exudate, texture and colour) largely depends on the size and location of the ice crystals formed [1–4]. Ice crystal size, shape, distribution and location in a given sample depend both on the number of ice nuclei formed in the early phase of the freezing process and on the rate of subsequent crystal growth [5]. The number of nuclei formed is considered to be directly proportional to the extent of supercooling (the temperature decreases under the equilibrium freezing point) before nucleation [6, 7]. When ice crystallization occurs, the temperature of the system quickly rises back to this equilibrium point, due to the release of latent heat, and crystal growth takes place by incorporation of water molecules to these nuclei at the equilibrium temperature.

One of the main factors determining the speed of growth is the rate of heat removal from the system. Slow freezing enhances the formation of large extracellular ice crystals, which cause damage in food products, particularly in cellular (muscle or vegetable) tissues [8–10]. Lower heat dissipation rate gives rise to fewer initial nuclei, which grow "freely" (with little competition for space with other nuclei) and mainly in the extracellular regions, and less concentrated in solutes. Ice crystals may mechanically tear cells membranes and walls and other tissular structural elements. Nevertheless, damage through cytoplasm dehydration is considered to be more important in cellular foods [11]. Water is extracted from cells if extracellular freezing occurs and the cellular membrane may be irreversibly damaged. Upon thawing, important quality losses can be

observed that can be related to these membrane alterations and water migration. The quicker the freezing process, the higher number of nuclei will be formed, and, while the chance of intracellular nucleation increases, higher quality can be expected in the final thawed products.

In the classical freezing process (CF), at atmospheric conditions, nucleation only occurs near the sample surface, in direct contact with the cooling medium, where high extents of supercooling are reached. When the latent heat of crystallization is removed, ice crystals grow from their initial location at the sample surface towards the centre, giving rise to final needle-shaped and radially oriented crystals. When small products (e.g., peas, shrimps, etc.) are frozen, high freezing rates can be achieved, the ice crystals formed are small and the quality of the end product is well preserved. The opposite occurs in large products, in which only low freezing rates can be achieved and steep thermal gradients are created due to slow thermal dissipation. Therefore, large ice crystals are formed, which produce detrimental effects.

Recrystallization

Temperature fluctuations during storage and transport of frozen products are known to induce increases in the mean crystal diameter and to reduce the number of crystals, since temperature elevations melt the smaller crystals while temperature decreases lead to growth of the larger ones. Therefore, isothermal conditions are essential to preserve the quality and extend the shelf life of frozen foods. But, even at isothermal conditions (when the total amount of ice remains constant in the frozen product), the originally formed ice crystal distribution is unstable, as the ice–liquid water interface tends to be minimized. Recrystallization, the process of reduction of the number of molecules forming the interface, includes a number of phenomena that involve changes in the number, size, shape, orientation or perfection of the ice crystals after their initial creation [12].

Several types of recrystallization processes, relevant to frozen food, have been described in the literature [12–17], amongst them, isomass recrystallization, accretion and migratory recrystallization. Isomass recrystallization (rounding off) occurs in single crystals and consists of changes in their surface or internal structure, so that crystals with irregular shapes and large surface-to-volume ratios assume more compact structures, without overall mass changes. In this way, sharper surfaces, less stable than flatter ones, become smoother over time. Accretion refers to the tendency of crystals in close contact to fuse together. Migratory recrystallization (also called Ostwald ripening when it takes place at constant temperature and pressure) refers to the tendency of larger crystals to grow at the expense of the smaller ones without physical contact between them.

Theoretical discussions of ice recrystallization in food systems have been based generally on Ostwald ripening principles [18–22]. Most models adopt a general time-dependent solution to predict the evolution of the mean size of the ice crystal population with time:

$$\bar{r}^n = \bar{r}_0^n + K \cdot t \qquad (1)$$

where $\bar{r}$ is the mean ice crystal radius at any time t, $\bar{r}_0$ is the mean initial crystal size, K is the recrystallization rate constant and n is a parameter that depends on the mechanism, which limits the recrystallization process [16]. Two steps can be identified in crystal growth through Ostwald ripening: water molecules diffusion by mass transfer and incorporation to the ice structure at the interface, crystal–solution. The exponential factor n has a value of 2 when surface incorporation is the limiting step [23] and also when ripening is limited by convective molecular diffusion, which occurs in systems with fluid flow. For ripening limited by bulk molecular diffusion in a stagnant solution (non-convective diffusion), which is analogous to migration of water molecules through the unfrozen phase, $n = 3$ [14, 15].

The recrystallization rate, K, can be obtained from Eq. (1) as the slope of the plot of $\bar{r}^n$ versus time, and consequently, its dimensions correspond to the model applied. Its value depends also on the size parameter employed (i.e., the radial constant, as defined here, must be multiplied by n^2 to work with diameters). The recrystallization rate increases with temperature. Its effect on the kinetic constant can be expressed by means of an Arrhenius-type dependence [23, 24]. Many factors influence the recrystallization rate at isothermal conditions, mostly through the initial ice crystal distribution. Besides the product composition, the freezing process and the storage temperature are the most important. The freezing process characteristics determine the initial number, size, shape, orientation and spatial distribution of the crystals formed. Those processes resulting in the formation of a high number of small ice crystals are reported to provide maximum stability against recrystallization [16].

HPSF

During the past decade, high-pressure shift freezing (HPSF) has been envisaged as a promising food freezing method, mainly due to its potentiality for reducing the thawing time and improving the characteristics of the ice crystals formed [5, 8, 25–30]. High-pressure shift freezing (see scheme in Fig. 1) takes advantage of the anomalous temperature/pressure phase diagram of water in the region of ice I to achieve high extents of supercooling, which increase the probability of ice nucleation. In this process,
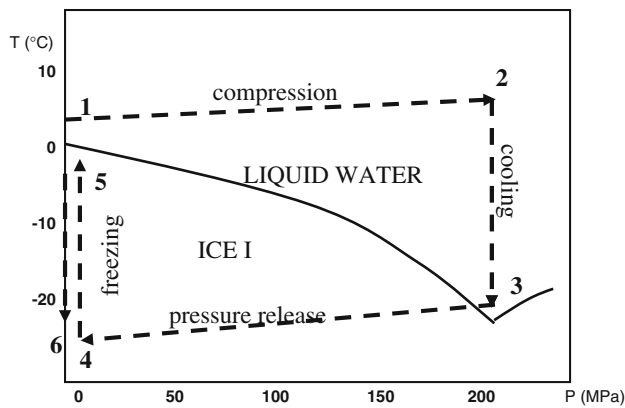
Fig. 1 Schematic diagram of the high-pressure shift freezing process: process path (*broken line*); pure water pressure–temperature phase diagram (*straight line*)

pressure is first increased (steps 1–2) and then the sample is cooled (under pressure) below 0 °C, while water remains unfrozen, following the corresponding phase diagram (steps 2–3). Once the target temperature is reached (point 3), pressure is quickly released (steps 3–4), which, due to the isostatic nature of pressure, induces a high uniform supercooling degree in the sample (point 4). This super-cooling causes uniform formation of ice nuclei throughout the sample (regardless of its shape and size) and not only on its surface, as it happens in conventional freezing. After nucleation, latent heat is released and the sample temper-ature rises to the corresponding freezing point (steps 4–5). Freezing is then completed at atmospheric pressure (steps 5–6). The higher the pressure and the lower the temper-ature before expansion, the more ice is formed, and hence the shorter is the phase transition time for a given cooling temperature [31, 32]. Many studies in the literature show that ice crystals formed by this procedure are granular in shape with no specific orientation and are dispersed throughout the whole sample, demonstrating that during the expansion phase, ice nucleation occurs homogeneously and not only on the sample surface. HPSF nucleation has been shown to occur not only in the extracellular medium, but also in the intracellular regions [3, 9]. The ice crystals formed by HPSF have also been reported to cause con-siderably less damage to food than those produced by conventional freezing [1–3, 9, 10, 27–30].

To preserve the benefits of HPSF during long periods of time, it is essential to avoid the growth of the initial small ice crystals in frozen storage. However, only a few studies have been performed on this subject. Koch et al. [2] found that high-pressure shift frozen potato cubes had better quality than those conventionally frozen, but their subsequent fro-zen storage at −18 °C during 10 days resulted in quality deterioration, ascribed to Ostwald ripening. Conversely, Chevalier et al. [4] did not find any increase in the ice

crystals size of either HPSF or conventionally frozen turbot fillets after 75 days of storage at −20°C. These authors attributed their surprising results to the "relatively short" storage time and the isothermal conditions employed.

The objective of the present work is to investigate if high-pressure shift frozen systems follow the same ice recrystallization kinetics than those conventionally frozen (at atmospheric conditions). For this task, a purpose-built system, able to hold HPSF frozen samples of suitable size for microscopic observation without their alteration, was designed and built. The lack of convenient instrumental approaches may be the main cause of the lack of experi-mental data on crystal size behaviour. A high-pressure equipment was adapted to the freezing of these samples and the methodology for the evaluation of ice crystal growth was set up. Direct microscopic examination at different temperatures allowed to follow the evolution of ice crystals with time and to study the influence of the freezing method and storage temperature on recrystallization.

Materials and methods

High-pressure equipment

Freezing experiments were performed with a prototype high-pressure equipment (UNIPRESS, Warsaw, Poland) designed to work at pressures up to 700 MPa and temper-atures between −40 and 100 °C [33]. The high-pressure vessel, made of a copper–beryllium alloy, has an internal diameter of 30 mm, a height of 64 mm and a working volume of 45 mL. Silicone oil was used as the pressure and temperature transmitting medium. Pressure was generated by a high-pressure pump coupled to a high-pressure inten-sifier (Rexroth Bosch Group Ltd, Warsaw, Poland) and temperature was controlled by immersion in a bath fed by a cryostat. Three sheathed type-T thermocouples allowed to monitor the temperature at different points inside the vessel. Temperature and pressure were monitored by a Yokogawa DA100 data-gathering unit (Darwin, Yokogawa Electric Corp., Japan) interfaced to a personal computer, with a precision of 0.1 °C and 0.1 MPa, respectively.

Freezing of food model solution

A 1.86 N NaCl solution (Panreac, Madrid, Spain) prepared with deionized Milli-Q water (Millipore, Billerica, USA) was employed. This concentration was selected so that at −19.2 °C, the temperature at which the HPSF recrystalli-zation behaviour was to take place, the frozen water fraction was approximately 50%. Aliquots (<10 μl) were introduced in the chamber described below, for HPSF or atmospheric pressure immersion freezing. In the former,

samples were pressurized to 210 MPa and cooled down to −20 °C. Once equilibrium was reached, pressure was briskly released, inducing ice nucleation (see Fig. 1 as a guide, but in this case, due to the freezing point decrease caused by NaCl, the equilibrium freezing point was below 0 °C). Freezing was completed at atmospheric conditions. Freezing at atmospheric pressure (APF) was performed by immersion in silicone oil inside the high-pressure vessel kept at −20 °C. In both cases, thermocouples in close contact with the chambers showed that thermal equilibrium with the surrounding cooling medium was attained within seconds (data not shown). The freezing rate, the ratio of the difference in initial and final temperatures to freezing time [34], is a determinant parameter for ice crystal size. Nevertheless, due to the small sample size, freezing rate determination was considered to be too inaccurate. Approximate values greater than 20 °C/s could be estimated. All the experiments were at least duplicated.

Microscopic ice crystal observation

Observations were carried out with an Olympus BX41 microscope (Olympus, Tokyo, Japan), using transmitted light and UPLAN FL 4X, 10X and 20X Olympus and Nikon (Kanagawa, Japan) 20X objectives (depending on the particular crystal size of each sample). The microscope was fitted with a PE120 Peltier-based cooling stage coupled to a PE 94 temperature control system (Linkam Scientific Instruments, Waterfield, UK), allowing temperature control down to −25 °C.

Once the observation chambers were located over the cooling stage, temperature was raised from −19.2 °C, the lower attained at the chamber, to the target experimental temperature and kept constant for a period of 3 h to study recrystallization phenomena, a period considered enough to represent the more intense phase of the recrystallization process. These temperatures were −19.2 °C for comparison of HPSF and APF frozen samples and −9.5, −12.4, −14.3 and −19.2 °C for the system test temperature dependence study.

The evolution of the ice crystals during this period was followed by the study of the micrographs that were automatically taken at 10-minute intervals with an Olympus DP70 microscope camera (Olympus, Tokyo, Japan), interfaced to a personal computer. They were analysed using an image analysis software (AnalySIS FIVE, Soft Imaging System GmbH, Münster, Germany) which is able to detect crystal boundaries, although the operator is often required to "round" and identify crystals. For each case considered, not less than 100 ice crystals were initially identified by the programme (typically 150–200 initial crystals, which become 40–50 after the observation period). The corresponding area (A) and equivalent diameter

(D_{eq}), defined as the diameter of a circle with the same area than the actual area measured in the ice crystal, were determined. Roundness (Rd) was also calculated to evaluate the shape of the ice crystals as

$$Rd = \frac{4 \cdot \pi \cdot A}{P^2} \tag{2}$$

where P is the perimeter. The roundness gives a value between 0 and 1, the latter corresponding to a sphere.

Statistical analysis

The results were statistically analysed and significant differences were determined by variance analysis (ANOVA) for a 95% confidence level using SPSS 12.0 software (SPSS Inc., Chicago, IL, USA). Differences between means were resolved by a Duncan test for multiple comparisons.

Results and discussion

Design of the observation chamber

The observation of ice samples produced under hydrostatic pressure is problematic, especially without alteration of the ice fraction and crystal size distribution. Pressure is transmitted by a liquid medium, which, both for the adequate isostatic transmission of pressure and the extraction of the sample, must be fluid at all experimental temperatures. The sample to be observed must, so, be separated from this fluid and it must be possible to extract it from the pressurization vessel and place on the cold microscope stage with no alteration or fluid contamination [35]. Systems based on the pressurization of a chamber small enough to allow microscopic observation are adequate to study the instantaneous ice formation process, but the evolution of the crystal size distribution in the growing process would be lost, as it depends on the macroscopic temperature and heat dissipation characteristics. Finally, breaking of larger portions, though fully incorporating the growth effect, is not viable, as the cutting or breaking process may produce local temperature increases that would alter the initial ice distribution.

To avoid resorting to indirect methods, such as freeze-drying [28] or freeze-substitution [9, 24], a small chamber suitable for its microscopic observation was designed and built in collaboration with UNIPRESS (Polish Academy of Sciences, Warsaw, Poland) (Fig. 2a). The chamber has an optical path of approximately 0.8 mm, maintained by a rubber gasket between two rings screwed together and keeping two optically flat sapphire windows attached to the gasket, ensuring hermetic closure. Several holes in the brass frame allow equilibrium of the inner and outer pressures.
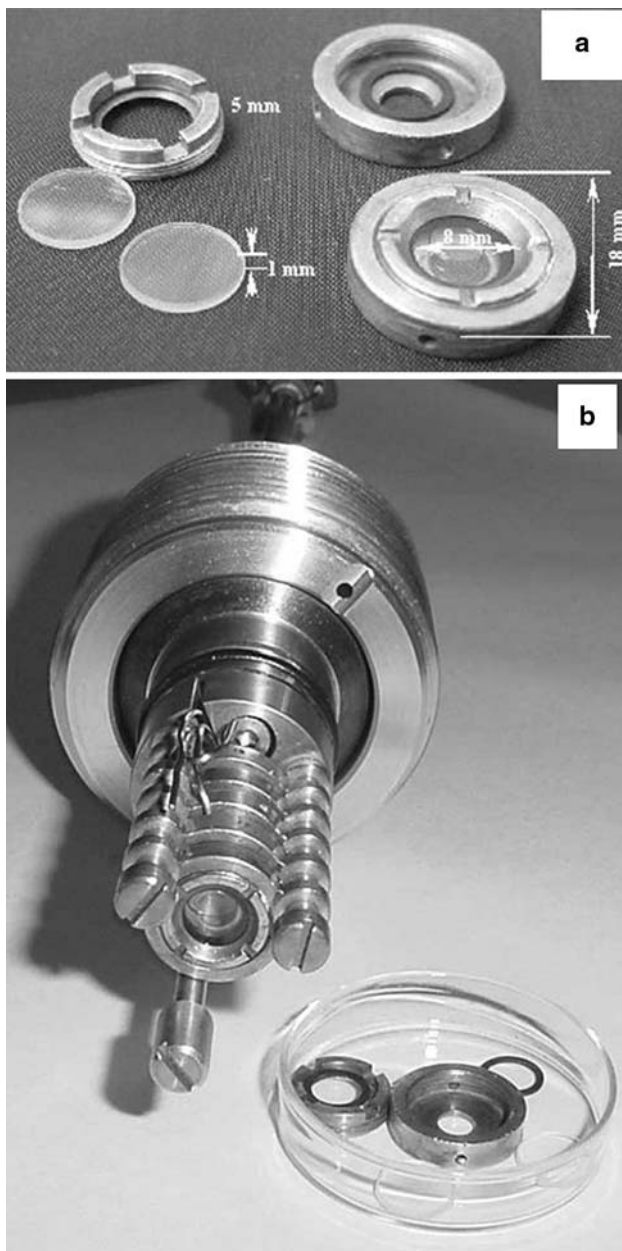
Fig. 2 **a** Cells for microscopic observation specifically designed for working under pressure. **b** Special holder designed to place six cells at defined positions inside the vessel

When the ice crystal size is particularly small, the microscope light beam must cross a large number of interfaces (water–ice and ice–ice). Observation can be difficult or even impossible, as a large part of the light beam becomes dispersed. To minimize this problem, the path length in these cells (the space between sapphire plates, occupied by the sample) is reduced as much as possible. This procedure allows the observation of most ice crystal samples.

A holder attached to the upper plug of the pressure vessel (Fig. 2b) allows quick extraction of the chambers and parallel experimentation, while the temperature can be monitored at several points in the chambers through thermocouples. The thickness of the upper ring was the minimal possible, to reduce the observation distance as much as possible, in spite of the relatively thick windows. The angle of the frame was designed so that a 20X Nikon objective could work at a correct focus distance. The copper–beryllium material of the cells ensured good thermal contact with the microscope cooling stage.

These observation chambers are also suitable containers for classical freezing, either by contact, air flow, immersion or cryogenic processes, allowing easier comparison of ice distribution, strongly dependent on sample size and distance to surface.

The procedure involves, once freezing is complete, extraction of the holder from the high-pressure vessel and quick release of the chambers in a Dewar flask filled with liquid nitrogen, which stops the ice crystals size evolution till their microscopic observation. Then, chambers can be transferred to the microscope stage preset at the desired temperature. The actual chamber temperature is slightly different from that read by the microscope stage (designed for smaller flatter samples). So, a thin T-thermocouple inserted in the cell ring is used to monitor the actual temperature. When necessary, a jet of nitrogen gas, cooled by passage through a refrigeration coil, is directed towards the microscope objective to avoid condensation. A glycerol drop prevents frost formation on the cell surface.

Test of the recrystallization measurement system

To test the full observation system (chamber, microscope, stage, camera and image analysis system) the recrystallization of immersion frozen samples of 1.86 N NaCl aqueous solutions was studied. Table 1 shows the size evolution data obtained at different temperatures for this system. The temporal size evolution can be fitted to both quadratic and cubic models after Eq. (1) using both $n = 2$ and $n = 3$ values, but the relative quality of the fit changes with the observation temperature (Table 1). The higher the temperature at the cryo-stage, the larger would be the fitted recrystallization constants (K), in good agreement with other authors observations [14, 15, 23, 24]. The effect of temperature on K can be expressed by means of an Arrhenius-type dependence as

$$K = K_0 \cdot e^{-E_a/RT_k} \tag{3}$$

and

$$\ln K = \ln K_0 - \frac{E_a}{RT_k} \tag{4}$$

where K_0 is a pre-exponential factor (with the same units as K), E_a (J/mol) the energy of activation, R (J/mol/K) the universal gas constant and T_k (K) the absolute temperature.

Table 1 Radial recrystallization constants (K) obtained from Eq. (1) for exponents $n = 2$ and $n = 3$, with their fit-quality indexes and average error, ice molar fraction, solute concentration at the liquid phase and dynamic viscosity of the solution at the different storage temperatures

Temperature (°C)	$n = 2$ K (µm²/min) R^2; $\sum E^2/n$ (µm²)	$n = 3$ K (µm³/min) R^2; $\sum E^2/n$ (µm²)	χ_{ice}	C (%)	μ (10^{-3} Pa s)
−9.5	9.97	469	0.1963	13.5	3.2
	0.92; 9.2	0.81; 24.5			
−12.4	6.82	302	0.3464	16.6	3.6
	0.97; 2.47	0.94; 4.33			
−14.3	5.47	205	0.4087	18.4	4.6
	0.96; 2.39	0.992; 0.55			
−19.2	2.47	55.9	0.5054	22.0	6.5
	0.94; 2.91	0.93; 2.57			

R^2: Quality of the fit

$\sum E^2/n$: Average error (average squared difference between experimental and calculated radius)

χ_{ice}: Ice fraction

C: w/w sodium chloride concentration at the liquid phase

μ : Liquid phase dynamic viscosity (data approximated by a simple interpolation from [36])

Figure 3a, b shows the logarithmic values of the quadratic [ln K (µm²/min)] and cubic [ln K (µm³/min)] fitted constants plotted versus T_k^{-1}. The corresponding activation energies of grain growth (E_a) were determined from the slope of the plots. The obtained values (7.0×10^4 and 10.7×10^4 J/mol for $n = 2$ and $n = 3$, respectively) were close enough to the value of $E_a = 11.64 \times 10^4$ J/mol, reported by Martino and Zaritzky [23, 24] for measurements of the growth rate on 0.28 N NaCl frozen solutions maintained at different temperatures.

In the experimental time considered (up to 3 h), ice crystal size evolution fits using $n = 2$ or $n = 3$ are practically equivalent (the maximum difference in the crystal size calculated by the two methods being 5 µm). Nevertheless, even at these short times, it is found that in samples kept at the higher temperatures (−9.5 and −12.4 °C), better results were obtained for $n = 2$ (higher values of the correlation coefficient, R^2, and lower average error, $\sum E^2/n$), while at the lower ones (−14.3 and −19.2 °C), $n = 3$ gave equal or even better fittings. A suitable explanation is that at high temperatures, the recrystallization process is limited by the rate of incorporation of water molecules to the crystal lattice (surface reaction). As the storage temperature decreases, the migration of water molecules in the unfrozen phase is hindered and bulk diffusion acquires importance as limiting mechanism for recrystallization. At the lower temperatures, the viscosity of the unfrozen phase of the sample is high (Table 1) (data approximated by a simple interpolation from [36]).

HPSF vs. APF recrystallization

To avoid possible errors resulting from variations in the initial conditions, HPSF samples were studied at a
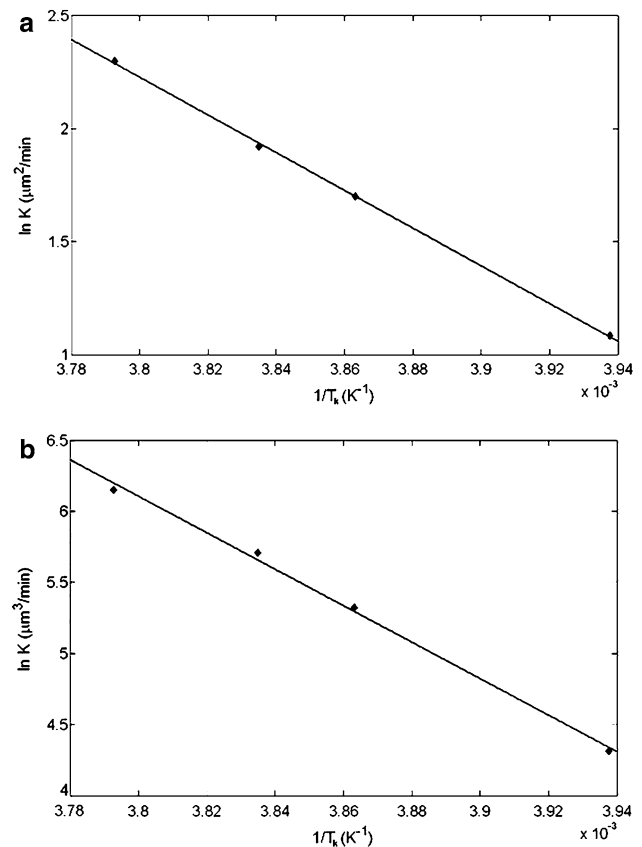

Fig. 3 Effect of temperature on the radial recrystallization rate. K values obtained considering $n = 2$ (**a**) or $n = 3$ (**b**) in Eq. (1)

temperature close to that of the original freezing process, to avoid changes in frozen water fraction and initial ice size distribution, as well as unfrozen phase solute concentration.

The HPSF process has been reported to be more efficient at the maximum supercooling degree, (i.e., that generated in an expansion from 210 MPa and −20°C to atmospheric pressure) (see Fig. 1 as a guide, but the equilibrium freezing point is below 0 °C here) [31]. Table 2 shows the experimental and derived data of the HPSF process. In an adiabatic expansion from a pressure of 210 MPa to atmospheric conditions after equilibration at −20°C, the supercooling degree generated (for the whole of the sample) is 13.1 °C, calculated from the equilibrium freezing point of a 1.86 N NaCl solution and including the temperature decrease associated with depressurization [37]. This supercooling causes instantaneous freezing of over 15% of the water in the sample upon expansion. The rest of the ice (to the final equilibrium 51.56%) is formed by the growth of the initial crystals and depending on dissipation of heat to the cooling system, as the equilibrium freezing point decreases from the initial −7.19 to the −20°C final equilibrium conditions, corresponding to a concentration of 22.4% NaCl (w/w). At this temperature and concentration, the viscosity of the solution was relatively high (data approximated by a simple interpolation from [36]), but, nevertheless, thermal equilibrium was quickly reached (data not shown).

Due to the relatively small sample size, the size of the immersion freezing ice crystals can be modulated and an initial sample size very close to that measured by HPSF was selected for comparison (Fig. 4). The latter figure shows a typical micrograph series of the time evolution of ice crystals obtained by the two freezing methods considered, at isothermal conditions (−19.2 °C). At time $t = 0$ min, both APF and HPSF samples (Fig 4a and d, respectively) showed a large number of small homogeneously distributed ice crystals that grew with time, as shown in Fig. 5. This figure presents the cumulative size distribution for both processes, which confirms the last observation. Most crystals (75% of the population) had a size ranging between 0 and 30 μm and there were no crystals larger than 50 μm, both in APF and HPSF samples. As time elapsed, the number of crystals decreased and their size increased appreciably due to recrystallization (Figs. 4, 5). All the recrystallization mechanisms working at isothermal

conditions were observed: accretion, isomass and migratory recrystallization. Images of some of these processes can be seen in Fig. 6. Figure 6a shows the final state after several accretion events had taken place, where crystal fusion had been observed (picture of the initial state not shown). Figure 6b, c shows a temporal sequence where an example of migratory recrystallization can be appreciated. At the initial times, recrystallization occurred via an accretive mechanism among close crystals, but isomass rounding and migratory recrystallization were dominant for longer times, when crystals were further apart, as observed by other authors [14]. After 2 h, the ice crystal evolution in APF and HPSF samples was apparently similar. In both cases, the number of crystals was reduced by, roughly, half and their mean equivalent diameter was doubled.

As above, the recrystallization constant was calculated for ice distributions resulting from both freezing processes (Table 3). Figure 7 shows a plot (for two single experiments) of the average ice crystal size of samples frozen by each procedure. It can be seen that the evolution of both samples is fairly parallel. The calculated fitted curves for both processes and $n = 2$ and $n = 3$ are also plotted. The fit quality R^2 helps to choose the best fit. HPSF samples at −19.2 °C render better fits for $n = 2$; hence, surface reaction appears as the limiting mechanism of recrystallization. Meanwhile, the quality and average fit errors of quadratic and cubic fits are similar for APF samples. This suggests some kind of morphological difference between the ice crystals formed by APF and HPSF, probably on their curvature or degree of perfection. The K obtained for both freezing processes were, within experimental error ($P < 0.05$), identical. Nevertheless, the plot in Fig. 7 indicates that there is little experimental evidence to distinguish between fits.

Regarding shape of crystals (Table 4), it was initially, for both freezing processes, rather circular (roundness was 0.64 ± 0.29 and 0.63 ± 0.35 for APF and HPSF, respectively) with no significant differences being found between samples ($P < 0.05$). In spite of this similar initial shape (similar roundness values), they grew following a different pattern, APF ice crystals became significantly less round with time than HPSF crystals (see also Fig. 4). Differences found in the APF and HPSF ice crystals shape evolution agree with the differences in best fitting n reported above, but more experimentation is needed to probe if these differences are maintained at longer storage times.

Recrystallization rate and real foods

As it is known, crystal size is always smaller in HPSF samples than in classical freezing [4, 9, 29, 30, 38]. But the crystals' actual size can be seen to vary widely, most likely depending on the actual food properties and constraints for

Table 2 Experimental and derived data of the HPSF process

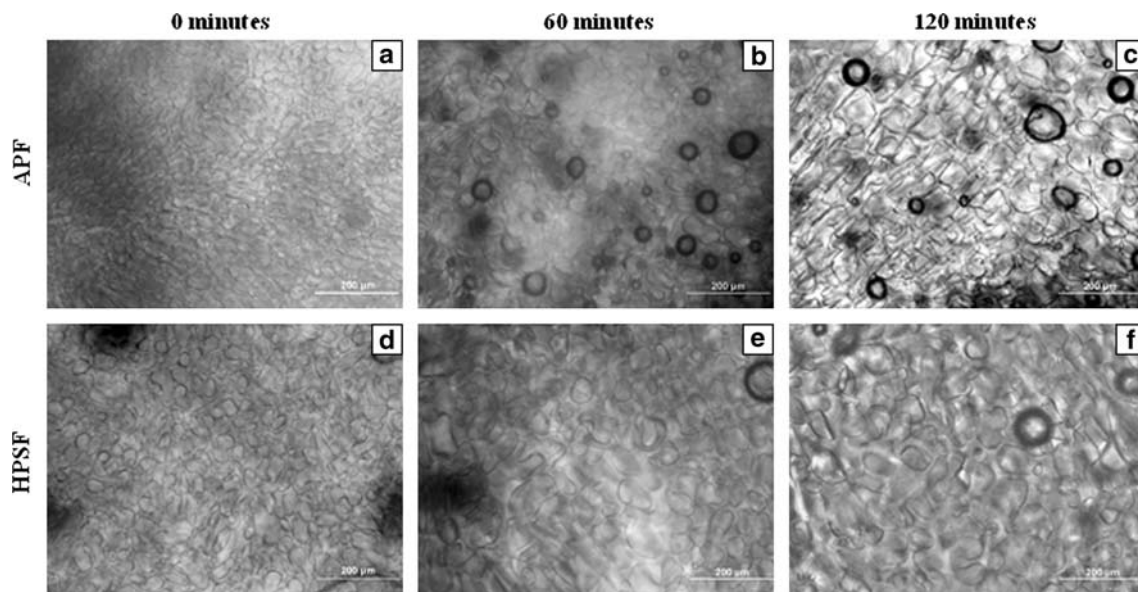|	
Pressure (MPa)	210
T (°C)	−20
Extent of supercooling (°C)	13.1
Instantaneous ice fraction after expansion[a]	0.1556
Ice fraction in equilibrium	0.5156
Concentration in the non-frozen phase (% w/w)	22.4
Dynamic viscosity (10^{-3} Pa s)	6.8
Freezing point (°C)	−7.19

[a] Calculated as described in [43]

Fig. 4 Light transmission micrographs showing a typical example of ice crystal growth in 1.86 N NaCl samples frozen either by immersion at atmospheric conditions (**a**–**c**) or high-pressure shift freezing (**d**–**f**), when kept at the microscope cooling stage at −19.2 °C for different time periods. White bar = 200 μm

Fig. 5 Time evolution of the cumulative distribution of ice crystals in 1.86 N NaCl samples frozen either by immersion at atmospheric conditions (*broken line*) or HPSF (*straight line*), when kept at the microscope cooling stage at −19.2 °C
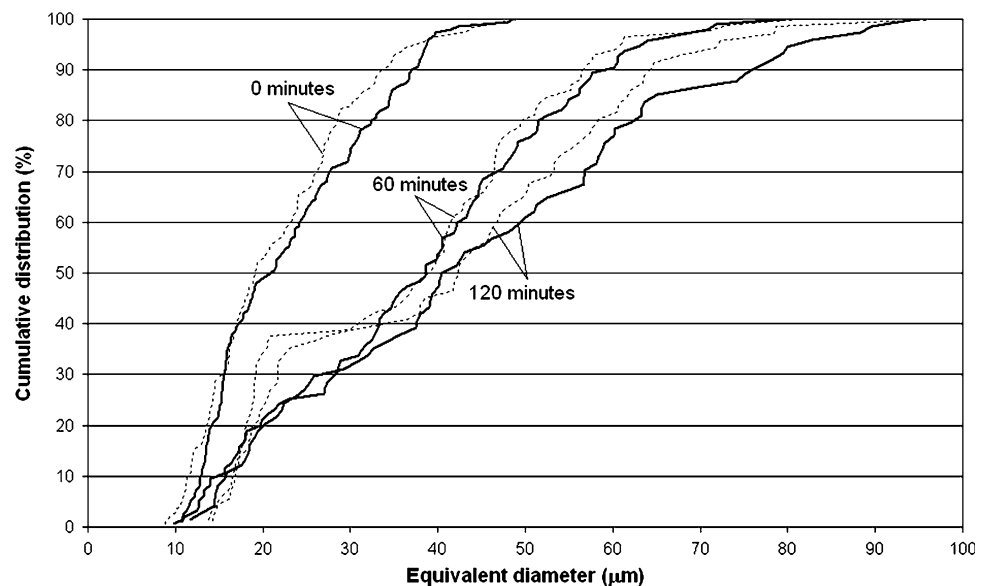
ice growth. A trend may be distinguished, so that those products with a weaker microstructure would allow the growth of larger crystals (e.g., 2% gelatin: 44 μm in HPSF vs. 120 in CF [29], fish muscle: 20 μm/HPSF vs. 60 μm/CF [4], tofu: 20 μm HPSF vs. 40–60 μm/CF [38]), while those with more and stronger structural elements would limit the ice crystal growth, showing finally smaller crystals (e.g., 10% gelatin: 6 μm/HPSF vs. 200 μm/CF [30], pork muscle: 2–4 μm/HPSF vs. 20–30 μm/CF [9]). In this way, gelatin samples show larger ice crystals for the lower concentration were gelatin filaments would be more separated. Additionally, soluble substances would also play a role, limiting crystal growth through viscosity changes, as it is shown in the case of trehalose [38], and may be modifying mechanisms, as suggested above. All those effects would work in a similar way for HPFS or classically frozen products.

In our experiments, HPSF ice crystals had a size corresponding to those products with less structural constraints (2% gelatin [29]), which may imply that the sodium chloride model solution employed is similar in behaviour to those foods with little opposition to ice growth. As mentioned earlier, both mechanisms of damage to food structure and quality, i.e., mechanical damage to membranes and

Fig. 6 Micrographs showing examples of recrystallization mechanisms during the storage of high-pressure shift frozen samples at −19.2 °C: **a** accretion recrystallization (initial, separate crystal state, not shown); **b** and **c** migratory recrystallization. (The time lapse between **b** and **c** was 5 min)
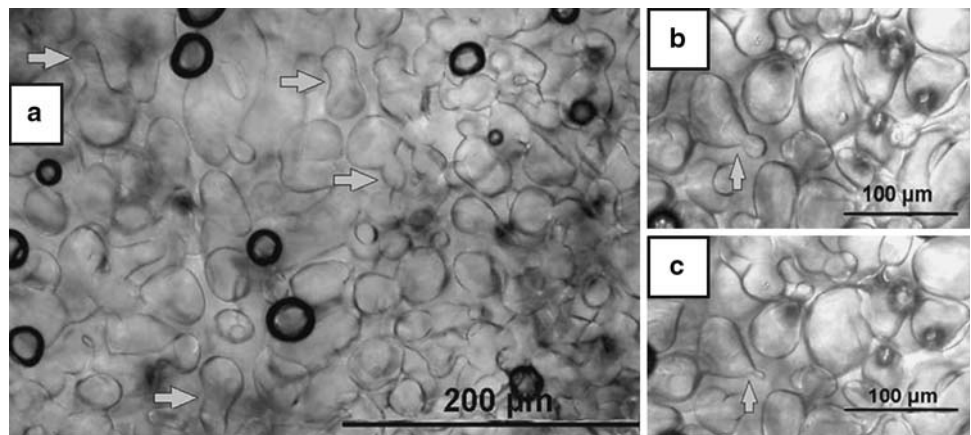
Table 3 Radial recrystallization constants (K) obtained from Eq. (1) for $n = 2$ and $n = 3$ for the high-pressure shift freezing (HPSF) and atmospheric pressure freezing (APF) samples stored at −19.2 °C, with their fit-quality indexes and average errors

−19.2 °C	$n = 2$ K (µm²/min) R^2; $\sum E^2/n$ (µm²)	$n = 3$ K (µm³/min) R^2; $\sum E^2/n$ (µm²)
APF	2.47	55.9
	0.94; 0.54	0.93; 0.50
HPSF	2.78	74.7
	0.82; 2.91	0.79; 2.57

R^2: Quality of the fit

$\sum E^2/n$: Average error (average squared difference between experimental and calculated radius)

Fig. 7 Ice crystals evolution with time in 1.86 N NaCl samples frozen by APF (*filled square*) and HPSF (*open triangle*) when kept at the microscope cooling stage of −19.2 °C for 3 h: *straight line* quadratic, $n = 2$, model fit; *dots* cubic, $n = 3$, model fit

Table 4 Mean roundness (Rd) ± standard deviation of ice crystals in APF and HPSF samples at different times, which show their shape evolution with time

	0 min	60 min	120 min
APF samples	0.64 ± 0.29abc	0.60 ± 0.37bc	0.56 ± 0.36c
HPSF samples	0.63 ± 0.35 abc	0.71 ± 0.29a	0.68 ± 0.33ab

Different letters, both in columns and rows, indicate significant differences between treatments and times (Duncan test for multiple comparisons, $P < 0.05$)

structural elements and cellular damage through dehydration, would be dependent on the ice crystal size and its evolution during storage. Consequently, the advantages gained from a more expensive or involved freezing method such as HPSF would be lost during storage if recrystallization phenomena increase this initial size to values close to that of classical freezing. The observation period considered in this study (3 h) does not allow proper differentiation between crystal growth models. They were chosen for methodological requirements, as the error related to the number of observed crystals increased dramatically and was reduced with longer times. The ice crystal size distribution attained after much longer storage times would be drastically different for both models.

Application of the model considered with the constants determined here (Table 3) might mean that, in a relatively short time period, the HPSF benefits would be completely lost, as the procedure is quite insensitive to the initial dimensions of the crystal. The time scale in which recrystallization damages real frozen foods is quite variable [15]. Most data correspond to foods with some structural elements, likely to limit this process and, moreover, real storage often includes temperature fluctuations that would make comparison even more difficult. Ice cream was reported to deteriorate after 2 weeks (storage at 13.3 °C). Longer times were found at lower temperatures [39]. Other workers found an approximately 100% increase in the average crystal size for ice cream samples stored at −5 °C for nearly 7 h, approaching the size range were crystals organoleptically detected in ice cream (20–55 µm [40]) [15]. Model ice cream (sucrose solutions and stabilizer hydrocolloids) have been reported to suffer ice crystal size increases of 64–118% after complex temperature cycling

for 5 days [41]. A similar effect of restraint to free ice growth in real foods can be expected to take place during storage, as well as in the initial crystal growth period. Consequently, smaller recrystallization constants will have to be considered when predicting ice crystal size evolution for real systems. Moreover, when the "driving force" of initial crystal growth is much larger than that of recrystallization (latent heat as compared to small interfacial energy differences), the resistance of structural elements to ice growth may be more noticeable for recrystallization processes. In this case, if recrystallization rates are smaller in real systems, the initial ice crystal size will be a most important factor in the quality characteristics of frozen products. Martino and Zaritzky [24] formulated a recrystallization model that takes into account tissular structure limits and its application must be recommended to study the ice growth phenomena in real food.

A large number of parameters may have a marked influence over ice crystal behaviour at the microscopic scale. Such are local intra- and extracellular concentrations and flows of water and solutes, local viscosities and diffusion rates (both at molecular and ice crystal scales), availability of water bound to different components, even modulations of the ice–water interfacial energy by solutes. Further systematic study of is required for a better understanding of these phenomena.

The advantages of HPSF are not only limited to granting a smaller average crystal size. Apart from the additional benefits of reducing microbial load, which can contribute to expand frozen food self-life, the ice crystals generated by this procedure, irrespective of the average size, are not only extracellular but also intercellular, with the implications that the growth of these crystals would not cause the same degree of dehydration damage than extracellular ones. Also the spatial distribution of crystals is homogeneous, irrespective of the size of the sample. The real food data from the literature (e.g., [4, 9, 29, 30, 37]) have often been obtained with relatively small samples, while in the central regions of large food items the size generated by classical freezing can be much larger than those reported here.

The homogeneity of the size and shape distribution of ice crystals is also narrower for HPSF than for APF methods—see e.g., [3, 6, 42]. Also, their shape is generally rounder in HPSF. It must be remembered that these irregularities in distribution and shape are due to temperature gradients during freezing and that, given the small size of the samples considered here, the original size distribution was not very different for both procedures (this was intended, for optimal comparison purposes). Both a wide size distribution and shape irregularity are a source for increased recrystallization, as shown, for example, by [23], where those crystals with a smaller number of faces were found to have faster growth.

Conclusions

Similar recrystallization behaviour has been found for HPFS and APF frozen model samples. The simple model solution employed allowed ice crystals to grow in the absence of structural obstacles inherent to the cellular tissue of structured food and provided basic information on recrystallization mechanisms in APF and HPSF samples. But the obtained results may be not directly extrapolated to real structured food in which ice crystals tend to reach a limit size at long storage periods unlike in solutions where there are no steric hindrances to growth.

Further experimentation is needed to elucidate the mechanisms limiting recrystallization in HPSF and APF samples. The results obtained here suggest that ice crystals formed by high-pressure shift freezing are somehow morphologically different (probably in curvature or degree of perfection) to those formed by immersion at atmospheric conditions, but these preliminary results must be confirmed with studies on ice crystal evolution after longer storage times.

References

1. Fuchigami M, Kato N, Teramoto A (1996) Effect of pressure-shift freezing on texture, pectic composition and histological structure of carrots. In: Hayashi R, Balny C (eds) High pressure bioscience and biotechnology. Elsevier, Amsterdam, pp 379–386
2. Koch H, Seyderhelm WP, Kalichevsky MT, Knorr D (1996) Nahrung 40:125–131. doi:10.1002/food.19960400306
3. Sanz PD, Solas M, Otero L, de Elvira C, Carrasco JA, Molina-García AD (1998) Polish J Food Nutri Sci 7/48:65–68
4. Chevalier D, Sequeira-Muñoz A, Le Bail A, Simpson BK, Ghoul M (2001) Innovative Food Sci Emerging Technol 1:193–201. doi:10.1016/S1466-8564(00)00024-2
5. Thiebaud M, Dumay EM, Cheftel JC (2002) Food Hydrocolloids 16:527–545. doi:10.1016/S0268-005X(01)00133-3
6. Burke MJ, George MF, Bryant RG (1975) Water in plant tissues and frost hardiness. In: Duckworth RB (ed) Water relations of foods, Food science and technology monographs. Academic Press, New York, pp 111–135
7. Gilpin RR (1977) J Heat Transfer 99:419–424
8. Le Bail A, Chevalier D, Mussa DM, Ghoul M (2002) Int J Refrigerat 25:504–513. doi:10.1016/S0140-7007(01)00030-5
9. Martino MN, Otero L, Sanz PD, Zaritzky NE (1998) Meat Sci 50:303–313. doi:10.1016/S0309-1740(98)00038-2
10. Chevalier D, Sentissi M, Havet M, Le Bail A (2000) J Food Sci 65:329–333. doi:10.1111/j.1365-2621.2000.tb16002.x

11. Schmitt JM, Schramm MJ, Pfanz H, Coughlan S, Heber U (1985) Cryobiology 22:93–104. doi:10.1016/0011-2240(85)90012-4
12. Fennema OR (1973) Nature of the freezing process. In: Fennema OR, Powrie WD, Marth EH (eds) Low temperature preservation of foods and living matter. Marcel Dekker, New York, pp 151–239
13. Sutton RL, Evans ID, Crilly JF (1994) J Food Sci 59:1227–1233. doi:10.1111/j.1365-2621.1994.tb14683.x
14. Sutton RL, Lips A, Piccirrillo G, Sztchlo A (1996) J Food Sci 61:741–745. doi:10.1111/j.1365-2621.1996.tb12195.x
15. Donhowe DP, Hartel RW (1996) Int Dairy J 6:1191–1208. doi:10.1016/S0958-6946(96)00029-5
16. Hartel RW (1998) Mechanism and kinetic of recrystallization in ice cream. In: Reid DS (ed) Properties of water in foods: ISO-POW 6. Blackie Academic & Professional, London, pp 287–319
17. Flores AA, Goff HD (1999) J Dairy Sci 82:1408–1415
18. Lifshitz IM, Slyozov VV (1961) J Phys Chem Solids 10:35–50. doi:10.1016/0022-3697(61)90054-3
19. Wagner C (1961) Z Elektrochem 65:581–591
20. Kahlweit M (1975) Adv Colloid Interf Sci 5:1–35. doi:10.1016/0001-8686(75)85001-9
21. Jain SC, Hughes AE (1978) J Mater Sci 13:1611–1631. doi:10.1007/BF00548725
22. Williamson A-M, Lips A, Clark A, Hall D (1999) Faraday Discuss 112:31–49. doi:10.1039/a900710e
23. Martino MN, Zaritzky NE (1987) Sci Aliments 7:147–166
24. Martino MN, Zaritzky NE (1989) Cryobiology 26:138–148. doi:10.1016/0011-2240(89)90044-8
25. Cheftel JC, Lévy J, Dumay E (2000) Food Rev Int 16:453–483
26. Li B, Sun DW (2001) J Food Eng 54:175–182. doi:10.1016/S0260-8774(01)00209-6
27. Chevalier D, Le Bail A, Ghoul M (2000) J Food Eng 46:287–293. doi:10.1016/S0260-8774(00)00090-X
28. Zhu S, Le Bail A, Ramaswamy HS (2003) J Food Process Preservat 27:427–444. doi:10.1111/j.1745-4549.2003.tb00528.x
29. Zhu S, Ramaswamy HS, Le Bail A (2005) J Food Eng 66:69–76. doi:10.1016/j.jfoodeng.2004.02.035
30. Fernández PP, Otero L, Guignon B, Sanz PD (2006) Food Hydrocolloids 20:510–522. doi:10.1016/j.foodhyd.2005.04.004
31. Otero L, Sanz PD (2000) Biotechnol Prog 16:1030–1036. doi:10.1021/bp000122v
32. Otero L, Sanz PD (2006) J Food Eng 72:354–363. doi:10.1016/j.jfoodeng.2004.12.015
33. Guignon B, Otero L, Sanz PD, Molina-García AD (2005) Biotechnol Prog 21:439–445. doi:10.1021/bp049666d
34. Barbosa-Cánovas GV, Altunakar B, Mejía-Lorío DJ (2005) Freezing Fruits and Vegetables. FAO Agricultural Services Bulletin 158. FAO, Rome. http://www.fao.org/ag/ags/subjects/en/harvest/docs/ags_bulletins/freezing_of_fruits_and_vegetables.pdf
35. Molina-Garcia AD (2002) Biotechnol Gen Eng Rev 19:3–54
36. Kaufmann DK (1960) Sodium chloride. Acs monographs series no. 145. Reinhold, New York
37. Otero L, Molina-Garcia AD, Sanz PD (2000) Innovative Food Sci Emerg Technol 1:119–126. doi:10.1016/S1466-8564(00)00009-6
38. Fuchigami M, Ogawa N, Teramoto A (2002) Innovative Food Sci Emerg Technol 3:139–147. doi:10.1016/S1466-8564(02)00007-3
39. Earl FA, Tracy PH (1960) Ice Cream Trade J 56:36–37, 40, 42, 78–80
40. Hartel RW (1996) Trends Food Sci Technol 7:315–321. doi:10.1016/0924-2244(96)10033-9
41. Regand H, Goff D (2003) Food Hydrocoll 17:95–102. doi:10.1016/S0268-005X(02)00042-5
42. Kalichevsky MT, Knorr D, Lillford PJ (1995) Trends Food Sci Technol 6:253–259. doi:10.1016/S0924-2244(00)89109-8
43. Otero L, Sanz PD (2000) Biotechnol Progr 16:1030–1036. doi:10.1021/bp000122v S8756-7938(00)00122-3